thiocyanate–labeled sheep anti-mouse immunoglobulin G (Amersham, Buckinghamshire, UK) for light microscopy, or with FluoroNanogold anti-mouse Fab' fluorescein (Nanoprobes, Stony Brook, NY) for electron microscopy. All antibodies were diluted in the above-mentioned permeabilizing and blocking solution. Light microscopic analysis was performed by epifluorescent light microscopy (Axiophot; Zeiss, Oberkochen, Germany) or by confocal laser scanning microscopy (MRC-1000; Bio-Rad, Cambridge, MA). For analysis of confocal laser scanning microscope images, we used CoMOS software for image collection and qualitatively oriented image processing operations and MPL software for quantitatively oriented image processing operations. The sections labeled with FluoroNanogold anti-mouse Fab' fluorescein were detected by epifluoresence microscopy, fixed again in 1% glutaraldehyde with 0.2% tannic acid in phosphate buffer, rinsed with distilled water, and subsequently processed for silver enhancement in developer [30% gum arabic, 0.85% hydroquinone, and 0.11% silver nitrate in citrate buffer (pH 7.4)]; see Hayat (*27*) for detailed procedures. After enhancement, sections were stained with 1% uranyl acetate for 2 hours at room temperature. The samples were dehydrated in a graded series of ethanol concentrations and embedded in Epon 812. Ultrathin sections were cut on a conventional ultramicrotome, stained with uranyl acetate and lead citrate, and examined with a transmission electron microscope (1200EX; JEOL, Tokyo, Japan) at an accelerating voltage of 100 KV.

14. J. Eyer and A. Peterson, *Neuron* **12**, 389 (1994).
15. Y. Kanegae, M. Makimura, I. Saito, *Jpn. J. Med. Sci. Biol.* **47**, 157 (1994).
16. M. Staufenbiel, P. Epple, W. Deppert, *J. Virol.* **60**, 1186 (1986).
17. J. J. Blum and M. C. Reed, *Cell Motil. Cytoskeleton* **12**, 53 (1989); R. A. Nixon, in *The Neuronal Cytoskeleton*, R. D. Burgoyne, Ed. (Wiley-Liss, New York, 1991).
18. N. Hirokawa, *J. Cell Biol.* **94**, 129 (1982).
19. Virus-injected animals (*13*) were killed 2 days after infection; both proximal and distal nerve fragments from injected ganglia, each 2 mm in length, were isolated and homogenized in 100 μl PEM [100 mM Pipes (pH 6.9), 1 mM EGTA, 1 mM $MgCl_2$, 1 mM dithiothreitol, 1 mM phenylmethylsulfonyl fluoride, and leupeptin (100 μg/ml)] with 1% Triton X-100. Homogenates were resolved on a 7.5% SDS-polyacrylamide gel, electrotransferred onto a polyvinylidene difluoride membrane (Immobilon PVDF; Millipore, Bedford, MA), and probed with mAb to c-Myc and mAb to neurofilament M (NN18; BioMakor, Rehovot, Israel). The bound antibodies were detected with ^{125}I-labeled protein A (Amersham) and analyzed with an image analyzer (BAS 2000; Fuji, Tokyo, Japan).
20. S. Terada, T. Nakata, A. C. Peterson, N. Hirokawa, data not shown.
21. J. F. Engelhardt, X. Ye, B. Doranz, J. M. Wilson, *Proc. Natl. Acad. Sci. U.S.A.* **91**, 6196 (1994); B. R. Grubb *et al.*, *Nature* **371**, 802 (1994); Y. Yang *et al.*, *Nature Genet.* **7**, 362 (1994); Y. Yang *et al.*, *Proc. Natl. Acad. Sci. U.S.A.* **91**, 4407 (1994).
22. J.-P. Julien *et al.*, unpublished data.
23. H. Yamasaki, G. S. Bennett, C. Itakura, M. Mizutani, *Lab. Invest.* **66**, 734 (1992); O. Ohara, Y. Gahara, T. Miyake, H. Teraoka, T. Kitamura, *J. Cell Biol.* **121**, 387 (1993).
24. N. Hirokawa, *Trends Cell Biol.* **6**, 135 (1996).
25. ———, G. S. Bloom, R. B. Vallee, *J. Cell Biol.* **101**, 227 (1985).
26. I. Saito, Y. Oya, K. Yamamoto, T. Yuasa, H. Shimojo, *J. Virol.* **54**, 711 (1985); Y. Kanegae *et al.*, *Nucleic Acids Res.* **23**, 3816 (1995); S. Miyake *et al.*, *Proc. Natl. Acad. Sci. U.S.A.* **93**, 1320 (1996).
27. M. A. Hayat, *Principles and Techniques of Electron Microscopy* (CRC Press, Boca Raton, FL, 1989).
28. We thank I. Saito and Y. Kanegae (Institute of Medical Science, University of Tokyo) and J. Miyazaki (University of Tokyo School of Medicine) for supplying us with their recombinant adenovirus vector system and the CAG promoter, respectively. Their technical advice was essential for the successful construction of our vector. We also thank Y. Komiya and T. Tashiro (Gunma University School of Medicine) for their technical assistance and advice on the microinjection into dorsal root ganglia in vivo; S. Ijuin (Nippon Bio-Rad Laboratories) for his technical assistance in confocal laser scanning microscopy; H. Yorifuji (National Defense Medical College) for his guidance in electron microscopic procedures; J.-P. Julien (Montreal General Hospital Research Institute, Centre for Research in Neuroscience, McGill University) and R. Nixon (McLean Hospital, Harvard Medical School) for helpful comments on the manuscript and useful discussions; Y. Kobayashi (Kyorin University School of Medicine) and T. Funakoshi, S. Kondo, Y. Okada, and other members of the Hirokawa lab for stimulating discussions and invaluable advice throughout; and Y. Kawasaki, H. Sato, H. Fukuda, and Y. Sugaya for their technical and secretarial assistance. Supported by a Special Grant-in-Aid for Scientific Research from the Japan Ministry of Education, Science and Culture; a grant from the Institute of Physical and Chemical Research (RIKEN) to N.H.; a Grant-in-Aid for Scientific Research from the Japan Ministry of Education, Science and Culture to S.T.; and grants from the Medical Research Council of Canada and Muscular Dystrophy Association of Canada to A.C.P.

22 April 1996; accepted 10 June 1996

Immunodeficiency in Protein Kinase Cβ–Deficient Mice

Michael Leitges,*†‡ Christian Schmedt,* Rodolphe Guinamard, Jean Davoust, Stefan Schaal, Silvia Stabel, Alexander Tarakhovsky†

Cross-linking of the antigen receptor on lymphocytes by antigens or antibodies to the receptor results in activation of enzymes of the protein kinase C (PKC) family. Mice homozygous for a targeted disruption of the gene encoding the PKC-βI and PKC-βII isoforms develop an immunodeficiency characterized by impaired humoral immune responses and reduced cellular responses of B cells, which is similar to X-linked immunodeficiency in mice. Thus PKC-βI and PKC-βII play an important role in B cell activation and may be functionally linked to Bruton's tyrosine kinase in antigen receptor–mediated signal transduction.

Cross-linking of the antigen receptor on B and T cells by antigens or by antibodies to the receptor is accompanied by rapid phospholipase C–γ activation, resulting in phospholipid hydrolysis and subsequent activation of the serine-threonine–specific protein kinase C (PKC) (*1*). The term PKC defines a family of at least 10 proteins that are characterized by a high degree of homology in their catalytical and cysteine-rich domains. On the basis of structural similarity and the requirement of Ca^{++} or diacylglycerol (DAG) or both for catalytic activity, the PKC family has been subdivided into three groups. The Ca^{++}- and DAG-dependent PKCs are represented by PKC-α, -βI, -βII, and -γ isoforms; PKC-δ, -ϵ, -η, and -θ are DAG-dependent but Ca^{++}-independent; and PKC-ζ and -λ are not activated by Ca^{++} and DAG in vitro (*2*). Despite extensive information on the enzymatic properties and expression patterns of various PKC isoforms in cells of the hematopoetic system, little is known about the physiological role of individual PKC isoforms in lymphocyte function (*3*). We started to address this question with the analysis of the immune system of mice deficient for the Ca^{++}-DAG–dependent PKC-βI and -βII. Both PKC-β isoforms are encoded by the same gene and are expressed in B and T lineage cells (*4*).

The gene encoding PKC-β was disrupted in embryonic stem (ES) cells by insertion of a *lacZ-neo* cassette into the second exon of the PKC-β gene by homologous recombination (Fig. 1) (*5*). The presence of the targeted PKC-β allele in mice heterozygous or homozygous for the mutation was revealed by Southern (DNA) blot analysis (Fig. 1B). The absence of PKC-β protein in homozygous mutant mice was confirmed by protein immunoblot analysis of lysates of splenocytes and thymocytes (Fig. 1C) (*5*).

Analysis of lymphocyte populations revealed that the frequency and absolute number of the $CD23^-$ immunoglobulin M^+ (IgM^+) (B-1) B lymphocytes as well as of $CD5^+$ IgM^+ (B-1a) cells, which represent a substantial fraction of the B-1 lymphocyte population, were severely reduced in the peritoneal cavity of PKC-$\beta^{-/-}$ mice as compared with that of wild-type mice (Fig. 2) (*6*). B-1 lymphocytes are located predominantly in the peritoneal cavity of mice and are thought to belong to a separate B cell lineage that differs from those of other B

M. Leitges and S. Stabel, Max-Delbrück-Laboratorium in der Max-Planck-Gesellschaft, Carl-von-Linné-Weg 10, D-50829 Köln, Germany.
C. Schmedt, S. Schaal, A. Tarakhovsky, Institute for Genetics, University of Köln, Weyertal 121, D-50931 Köln, Germany.
R. Guinamard and J. Davoust, Centre d'Immunologie CNRS-INSERM de Marseille-Luminy, Case 906, 13288 Marseille Cedex 9, France.

*These authors contributed equally to this work.
†To whom correspondence should be addressed.
‡Present address: Max-Planck-Institut für Immunbiologie, Stübeweg 51, D-79108 Freiburg, Germany.

lymphocytes in surface marker expression, antibody repertoire, and signaling capacities (*7*). The frequency and absolute number of pre-B (IgM^- $B220^{lo}$ $CD43^-$) and mature (IgM^+ $B220^{hi}$) B cells in the bone marrow of PKC-$\beta^{-/-}$ and wild-type mice were essentially identical. Conventional B cells (IgM^+ $B220^+$ IgD^+ major histocompatibility complex class II^+ $CD43^-$ $CD5^-$) were present in the spleen and lymph nodes of PKC-$\beta^{-/-}$ and wild-type mice at similar frequency (Fig. 2). However, the absolute number of splenic B cells was slightly reduced from $29 \times 10^6 \pm 8 \times 10^6$ in wild-type mice to $20 \times 10^6 \pm 5 \times 10^6$ in PKC-$\beta^{-/-}$ mice. The thymuses of PKC-$\beta^{-/-}$ mice were of normal size and cellularity and contained $CD4^+$ $CD8^+$ double-positive cells and $CD4^+$ or $CD8^+$ single-positive cells at normal ratios. The lack of PKC-β did not alter the surface expression of the T cell receptor (TCR)–CD3 complex, CD5, heat-stable antigen, or CD69 on single-positive cells. $CD4^+$ and $CD8^+$ single-positive T cells were also present in the spleen and lymph nodes of PKC-$\beta^{-/-}$ mice at a frequency similar to that in wild-type mice.

B-1 lineage cells are known to be a major source of IgM and IgG3 antibodies in the serum (*8*). The levels of IgM and IgG3 in the sera of PKC-$\beta^{-/-}$ mice were strongly reduced as compared with those in wild-type mice and heterozygous mutants (PKC-$\beta^{+/-}$) ($P < 0.05$) (Fig. 3A) (*9*). This reduction may reflect the defect in the population of B-1 lymphocytes in PKC-$\beta^{-/-}$ mice. The titers of immunoglobulins of other isotypes were similar in PKC-$\beta^{-/-}$, PKC-$\beta^{+/-}$, and wild-type mice (Fig. 3A). The titers of IgM and IgG3 in sera of PKC-$\beta^{+/-}$ mice were slightly reduced when compared with those of wild-type mice, which may suggest a gene dosage phenomenon.

The changes observed in the immune system of PKC-$\beta^{-/-}$ mice match some of the features of X–linked immunodeficiency (XID) in mice (*10*). XID in mice is due to a single amino acid substitution of a highly conserved residue in the pleckstrin homology domain of Bruton's tyrosine kinase (Btk) (*11*). Human X-linked agammaglobulinemia (XLA) is also associated with mutations or deletions of the gene encoding Btk (*12*). A causative role of Btk in XID was confirmed by analysis of the immune system of mice homozygous for a targeted disruption of the Btk gene (*13*). Btk is expressed in B lymphocytes as well as in myeloid and erythroid cells and is implicated in antigen receptor–mediated signal transduction in B cells (*14*) as well as in the responses of B cells to stimulation via CD40, the interleukin-5 (IL-5) receptor, and CD38 (*15*). XID mice are characterized by a modest reduction in the population of splenic B cells, most of which exhibit an immature IgM^{hi} IgD^{lo} phenotype and a severe reduction of the population of B-1 cells (*16*, *17*). Furthermore, serum levels of IgM and IgG3 and humoral immune responses of conventional B cells to thymus independent–type II (TI-II) antigens are strongly reduced in XID mice (*16*). Primary antibody responses to T cell–dependent antigens in XID mice have been shown to be reduced as well, whereas secondary responses are largely unaltered (*17*).

To evaluate the degree of similarity between immunodeficiencies in PKC-$\beta^{-/-}$ and XID mice, we analyzed the immune responses of the PKC-$\beta^{-/-}$ mice to a T cell–dependent antigen, 4-hydroxy-3-nitrophenylacetyl (NP)–chicken γ-globulin conjugate (CG), and to a T cell–independent antigen, NP-Ficoll (*18*). PKC-$\beta^{-/-}$ mice were unable to mount a detectable humoral immune response against NP-Ficoll (Fig. 3B). In PKC-$\beta^{+/-}$ mice the responses were less than in wild-type mice, which supports the notion that the responses of B cells may depend on the PKC-β gene dosage. Primary antibody responses to both hapten (NP) and carrier (CG) were also significantly reduced in the PKC-$\beta^{-/-}$ mice immunized with NP-CG when compared with wild-type mice (Fig. 3C). In contrast, the amplitudes of the secondary immune response to NP in PKC-$\beta^{-/-}$ mice and wild-type mice did not differ significantly (Fig. 3C). The secondary immune responses to CG were less in PKC-$\beta^{-/-}$ mice than in wild-type mice (Fig. 3C).

Further similarities between PKC-$\beta^{-/-}$ and XID mice were revealed by analysis of in vitro proliferative responses of the PKC-$\beta^{-/-}$ B cells to various stimuli. B cells from

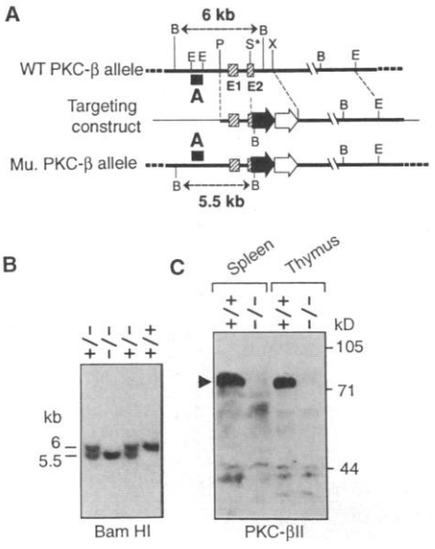

Fig. 1. Targeted disruption of the PKC-β gene. (**A**) Part of the wild-type (WT) PKC-β locus containing the first two exons E1 and E2, the targeting construct, and the mutant (mu.) PKC-β allele are shown. The PKC-β gene was disrupted by the insertion of the *lacZ* and *neo*^{r} genes (black and white arrows, respectively) at a Sal I site introduced into the second exon of the PKC-β gene by site-directed mutagenesis as described (*5*). The sizes of the two Bam HI fragments predicted to hybridize to diagnostic probe A (black box) are shown. Restriction enzymes are abbreviated as follows: B, Bam HI; E, Eco RI; P, Pvu II; X, Xba I; and S*, Sal I. (**B**) Southern blot analysis of genomic DNA. Genomic DNA was isolated from the tails of four littermates and was hybridized with probe A after digestion with Bam HI. (**C**) Immunoblot analysis of PKC-βI–βII. Immunoblots of splenocyte and thymocyte lysates from 129/Sv (+/+) and PKC-$\beta^{-/-}$ (−/−) mice were stained with polyclonal antibody to PKC-βII (*25*). The absence of PKC-βI in PKC-$\beta^{-/-}$ mice was also confirmed by immunoblot analysis with antibodies to PKC-βI. The position of PKC-βII is marked by an arrowhead.

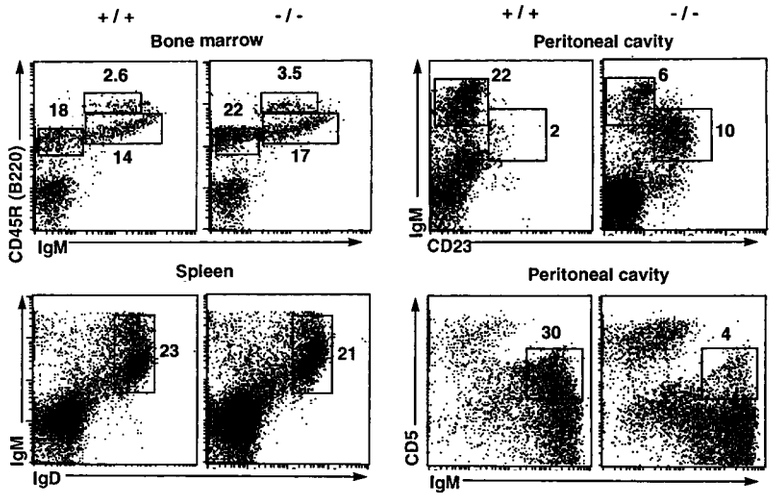

Fig. 2. Lymphocyte populations in PKC-$\beta^{-/-}$ mice. Representative flow cytometric analyses of mononuclear cells from lymphoid organs of 10-week-old PKC-$\beta^{-/-}$ and 129/Sv mice are shown (*26*). The percentages of the boxed cells within lymphocyte populations are indicated.

XID and Btk-deficient mice proliferate poorly in response to lipopolysaccharide (LPS) or antibody-mediated cross-linking of surface immunoglobulins IgM and IgD (*19*), whereas anti-CD40–mediated responses are either reduced or unaltered (*15*). The proliferation of PKC-$\beta^{-/-}$ B cells stimulated with an antibody to IgM was lower by a factor of 10 than the proliferation of wild-type B cells ($P < 0.001$) (Fig. 4A) (*20*). Compared with wild-type B cells, PKC-$\beta^{-/-}$ B cells were also characterized by less of basal proliferation in the absence of stimuli and were less responsive to stimulation with IL-4 or antibody to CD40 ($P < 0.005$ for each case) (Fig. 4A). However, the combined treatment of B cells with antibody to CD40 and with IL-4 resulted in

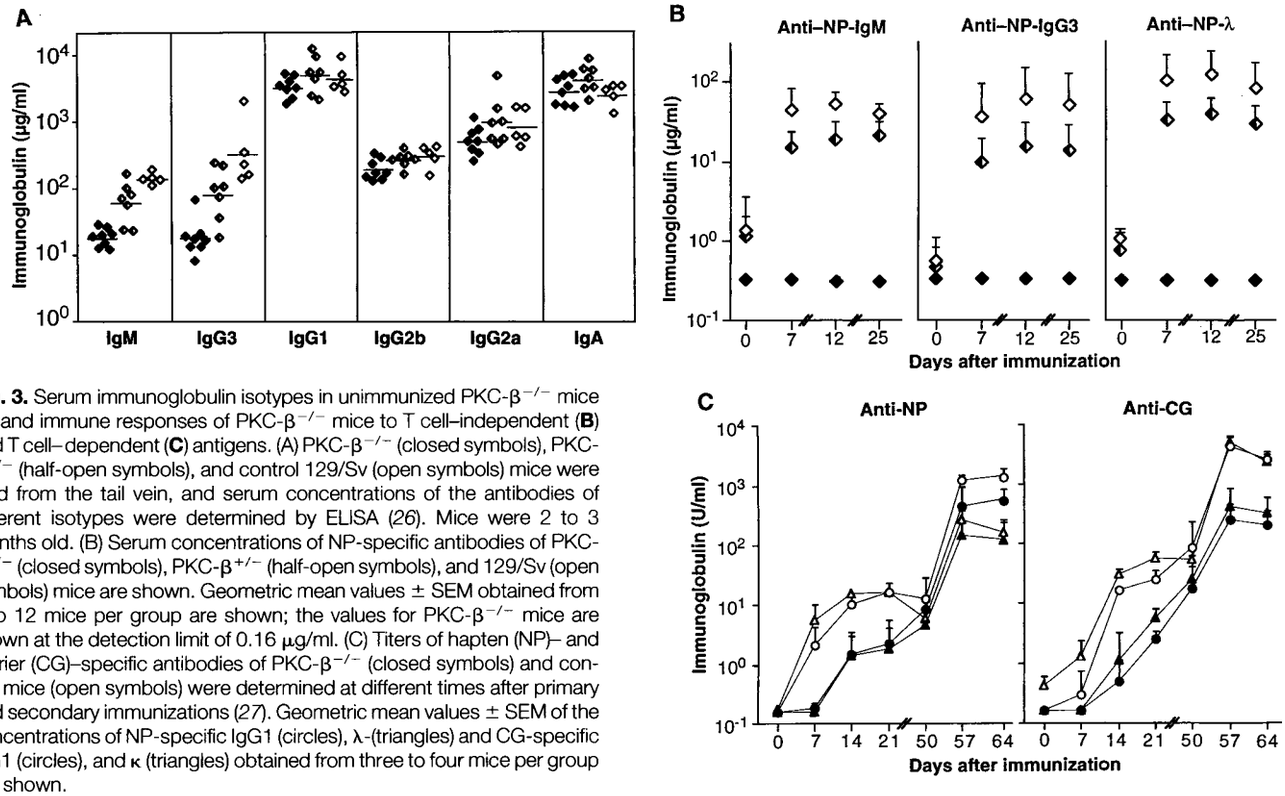

Fig. 3. Serum immunoglobulin isotypes in unimmunized PKC-$\beta^{-/-}$ mice (**A**) and immune responses of PKC-$\beta^{-/-}$ mice to T cell–independent (**B**) and T cell–dependent (**C**) antigens. (A) PKC-$\beta^{-/-}$ (closed symbols), PKC-$\beta^{+/-}$ (half-open symbols), and control 129/Sv (open symbols) mice were bled from the tail vein, and serum concentrations of the antibodies of different isotypes were determined by ELISA (*26*). Mice were 2 to 3 months old. (B) Serum concentrations of NP-specific antibodies of PKC-$\beta^{-/-}$ (closed symbols), PKC-$\beta^{+/-}$ (half-open symbols), and 129/Sv (open symbols) mice are shown. Geometric mean values ± SEM obtained from 8 to 12 mice per group are shown; the values for PKC-$\beta^{-/-}$ mice are shown at the detection limit of 0.16 μg/ml. (C) Titers of hapten (NP)– and carrier (CG)–specific antibodies of PKC-$\beta^{-/-}$ (closed symbols) and control mice (open symbols) were determined at different times after primary and secondary immunizations (*27*). Geometric mean values ± SEM of the concentrations of NP-specific IgG1 (circles), λ-(triangles) and CG-specific IgG1 (circles), and κ (triangles) obtained from three to four mice per group are shown.

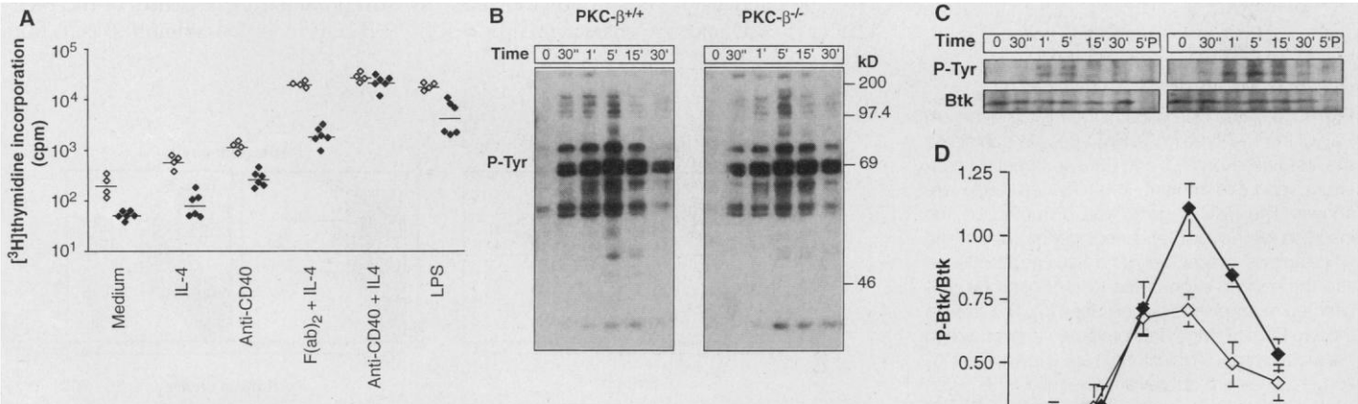

Fig. 4. In vitro responses of PKC-$\beta^{-/-}$ B cells. (**A**) Proliferative responses of B cells. Each symbol shows the amount of [^{3}H]thymidine [measured in counts per minute (cpm)] incorporated into the DNA of stimulated purified splenic B cells from 129/Sv (open symbols) and PKC-$\beta^{-/-}$ (closed symbols) mice (*26, 27*). Each dot represents the mean value of triplicate measurements in individual experiments. (**B** and **C**) Tyrosine phosphorylation (P-Tyr) of intracellular proteins in PKC-$\beta^{-/-}$ and control B cells. Purified splenic B cells were stimulated in vitro with antibody to IgM for the indicated periods of time, and phosphorylated proteins were revealed by protein immunoblot analysis of total cell lysates (B) or immunoprecipitates (C) obtained with an antibody to Btk (*22*). The symbol 5′P marks the lysates of B cells pretreated with the immunogenic Btk peptide during immunoprecipitation (*22*). (**D**) Kinetics of Btk phosphorylation in the wild-type (open symbols) and PKC-$\beta^{-/-}$ (closed symbols) B cells. The phosphorylation level of Btk and the amount of Btk in the immunoprecipitates from unstimulated and stimulated PKC-$\beta^{+/+}$ and PKC-$\beta^{-/-}$ B cells were determined by densitometric analysis. The ratio of phosphorylated Btk (P-Btk) over immunoreactive Btk (P-Btk/Btk ± SEM; $n = 3$), indicating the extent of tyrosine phosphorylation of Btk, was calculated for each time point.

an equally strong proliferative response of PKC-$\beta^{-/-}$ and wild-type B cells (Fig. 4A). Substantial variations in responses with a tendency toward hyporesponsiveness were observed in PKC-$\beta^{-/-}$ B cells stimulated with LPS (Fig. 4A). The responses of the PKC-$\beta^{-/-}$ B cells to the combined treatment with the phorbol ester PdBU and the Ca^{++} ionophore ionomycin, which are known to bypass B cell receptor (BCR)–dependent signaling, were similar to those of wild-type cells (*21*). This suggests an unaltered ability of PKCs other than PKC-β to be activated by PdBU and Ca^{++} in PKC-$\beta^{-/-}$ B cells. The reduction in antigen receptor–mediated proliferation in the absence of PKC-β is restricted to B cells, because the in vitro proliferation of wild-type and PKC-$\beta^{-/-}$ splenic T cells and thymocytes in response to antibody to CD3 alone or in combination with IL-2 was unaltered. This suggests the use of distinct PKC isoforms in BCR- and TCR-mediated signal transduction.

The impaired IgM-mediated proliferation of B cells indicates the existence of a downstream defect or defects in the BCR-dependent signaling cascade. However, the general pattern of BCR-induced tyrosine phosphorylation of intracellular proteins appears to be similar in PKC-$\beta^{-/-}$ and wild-type B cells (Fig. 4B) (*22*). The similarity between the immunodeficiencies in PKC-$\beta^{-/-}$ and XID or Btk-deficient mice points to a possible functional link between PKC-β and Btk in B cells. Indeed, an association between different PKC isoforms, including PKC-βI, and Btk has been shown in mast cells (*23*). Moreover, PKCs were found to phosphorylate and to inhibit the kinase activity of Btk (*23*). We found that levels of the IgM-induced tyrosine phosphorylation of Btk were higher in splenic PKC-$\beta^{-/-}$ B cells than in wild-type cells (Fig. 4, C and D). However, the catalytic activity of Btk in anti-IgM–stimulated PKC-$\beta^{-/-}$ and wild-type B cells was similar (*22*). These data argue against an involvement of PKC-β in the regulation of the catalytic activity of Btk but suggest a role for PKC-β in the transphosphorylation or dephosphorylation of Btk. The consequences of the increased tyrosine phosphorylation of Btk for the integrity of the BCR-dependent signal transducing chain, as well as the position of PKC-β relative to Btk in this chain, are unknown. An earlier study demonstrated that the defect in antigen receptor–induced proliferation of XID B cells could be overcome by a prolonged incubation of these cells with the potent PKC activator indolactam (*24*). This finding, combined with the known ability of Btk to interact with PKC-βI and our experimental data, would be in agreement with PKC-β being located in close proximity and downstream of Btk in the antigen receptor–dependent signaling pathway. The role of PKC-β in this pathway appears to be unique because it can not be replaced by other PKCs during T cell–independent activation of B cells. Therefore, the described role of PKC-β in B cell responses makes PKC-β an attractive target for immunomodulatory therapy using selective activators or inhibitors of this enzyme.

REFERENCES AND NOTES

1. E. Baixeras *et al.*, *Immunol. Rev.* **132**, 5 (1993); A. Weiss and D. R. Littman, *Cell* **76**, 263 (1994).
2. Y. Nishizuka, *Science* **258**, 607 (1992); H. Hug and T. F. Sarre, *Biochem. J.* **291**, 329 (1993); L. V. Dekker and P. J. Parker, *Trends Biochem. Sci.* **19**, 73 (1994); S. Stabel, *Semin. Cancer Biol.* **5**, 277 (1994); Y. Nishizuka, *FASEB J.* **9**, 484 (1995).
3. J. C. Cambier *et al.*, *Nature* **327**, 629 (1987); D. T. Francois *et al.*, *J. Immunol.* **140**, 3338 (1988); G. A. Koretzky, M. Wahi, M. E. Newton, A. Weiss, *ibid.* **143**, 1692 (1989); J. Freire-Moar, H. Cherwinski, F. Hwang, J. Ransom, D. Webb, *ibid.* **147**, 405 (1991); M. Szamel and K. Resch, *Eur. J. Biochem.* **228**, 1 (1995).
4. L. Coussens *et al.*, *Science* **233**, 859 (1986); Y. Ono *et al.*, *ibid.* **236**, 1116 (1987); H. Mischak *et al.*, *J. Immunol.* **147**, 3981 (1991); D. P. Cohen and T. L. Rothstein, *ibid.* **146**, 2921 (1991); D. Kelleher and A. Long, *FEBS Lett.* **301**, 310 (1992); N. Tarantino, P. Debre, M. Korner, *ibid.* **338**, 339 (1994).
5. The *lacZ-neo* cassette was inserted into the second exon of the PKC-β gene by homologous recombination. Details of the cloning and mapping of the PKC-β gene, electroporation of ES cells, selection of recombinants, generation of chimeric mice, and the analysis of expression of the PKC-β–β-galactosidase fusion protein in various tissues are described elsewhere (M. Leitges *et al.*, in preparation). Mice heterozygous for the disruption of the PKC-β gene were backcrossed to 129/Sv mice, and F_1 mice were bred to generate PKC-$\beta^{-/-}$ mice on a pure 129/Sv genetic background. For the analysis of PKC-β protein, spleens or thymuses of mice were disrupted on ice with a Dounce homogenizer in 50 mM tris-HCl (pH 7.5), 2 mM EDTA (pH 7.0), 10 mM EGTA (pH 7.0), 0.1% Triton X-100, 0.3% β-mercaptoethanol, phenylmethylsulfonyl fluoride (PMSF) (50 μg/ml), leupeptin (20 μg/ml), and aprotinin (20 μg/ml). After centrifugation for 20 min at 15000*g*, soluble proteins were separated on a 8.5% SDS-polyacrylamide gel and blotted onto nitrocellulose, and PKC-β protein was identified with PKC-β–specific antibodies (*25*) with the use of ECL reagents (Amersham).
6. Cells were stained with antibodies and analyzed by three-color flow cytometry on a FACScan (Becton Dickinson) (*26*). B and T ($CD4^+$ and $CD8^+$) single-positive cells in peripheral lymphoid organs and thymocytes were counted as described (*26*).
7. R. R. Hardy and K. Hayakawa, *Adv. Immunol.* **55**, 297 (1994); T. J. Kipps, *ibid.* **47**, 117 (1989).
8. L. A. Herzenberg *et al.*, *Immunol. Rev.* **93**, 81 (1986); I. Förster and K. Rajewsky, *Eur. J. Immunol.* **17**, 521 (1987).
9. Mice were bled from the tail vein, and the serum concentrations of different isotypes were determined by enzyme-linked immunosorbent assay (ELISA) as described (*26*). Data were evaluated by *t* test, with the use of Statistica software.
10. D. F. Amsbaugh *et al.*, *J. Exp. Med.* **136**, 931 (1972); I. Scher, A. K. Berning, R. Asofsky, *J. Immunol.* **123**, 477 (1979); I. Scher, *Adv. Immunol.* **33**, 1 (1982).
11. J. D. Thomas *et al.*, *Science* **261**, 355 (1993); D. J. Rawlings *et al.*, *ibid.*, p. 358.
12. C. I. Smith *et al.*, *Immunol. Rev.* **138**, 159 (1994); I. Vorechovsky *et al.*, *Hum. Mol. Genet.* **4**, 51 (1995).
13. W. N. Khan *et al.*, *Immunity* **3**, 283 (1995); J. D. Kerner *et al.*, *ibid.*, p. 301.
14. M. de Weers *et al.*, *Eur. J. Immunol.* **23**, 3109 (1993); S. J. Saouaf *et al.*, *Proc. Natl. Acad. Sci. U.S.A.* **91**, 9524 (1994); C. I. Smith *et al.*, *J. Immunol.* **152**, 557 (1994); Y. Aoki, K. J. Isselbacher, S. Pillai, *Proc. Natl. Acad. Sci. U.S.A.* **91**, 10606 (1994).
15. J. Hasbold and G. G. Klaus, *Eur. J. Immunol.* **24**, 152 (1994); S. Sato *et al.*, *J. Exp. Med.* **180**, 2101 (1994); L. Santos-Argumedo *et al.*, *Int. Immunol.* **7**, 163 (1995).
16. R. M. Perlmutter *et al.*, *J. Exp. Med.* **149**, 993 (1979); K. Haykawa, R. R. Hardy, L. A. Herzenberg, *Eur. J. Immunol.* **16**, 450 (1986).
17. J. J. Mond, Q. Vos, A. Lees, C. M. Snapper, *Curr. Opin. Immunol.* **7**, 349 (1995).
18. For the analysis of T cell–independent immune responses, mice were immunized intraperitoneally (i.p.) with 5 μg of NP_{24}-Ficoll in phosphate-buffered saline (PBS) and the serum concentrations of NP-specific IgM, IgG3, and λ-bearing antibodies were determined at different times after immunization (*27*). For the analysis of T cell–dependent immune responses, mice were immunized i.p. with 5 μg of alum-precipitated NP_{16}-CG. For the analysis of secondary immune responses, the same mice were reimmunized i.p. with 5 μg of NP_{16}-CG in PBS on day 50 after the primary immunization. The serum concentrations of NP- and CG-specific antibodies were determined at different times after immunization as described (*27*).
19. B. Huber and F. Melchers, *Eur. J. Immunol.* **9**, 827 (1979); J. J. Mond, M. Schaefer, J. Smith, F. D. Finkelman, *J. Immunol.* **131**, 2107 (1983); K. P. Rigley, M. M. Harnett, R. J. Phillips, G. G. Klaus, *Eur. J. Immunol.* **19**, 2081 (1989).
20. Splenic B cells were purified by depletion of non–B cells on MACS BS columns (Miltenyi Biotec, Bergisch Gladbach, Germany) as described (*26*) with the use of magnetic beads coupled to antibodies to CD43 (Miltenyi Biotec). B lymphocytes were stimulated by LPS (10 μg/ml), by antibody to CD40 (0.5 μg/ml) (Pharmingen) alone or in combination with IL-4 (5 U/ml) (Genzyme), or by AffiPure $F(ab')_2$ fragment goat anti-mouse IgM (2.5 μg/ml) (Dianova, Germany) as described (*26*). Data were evaluated by *t* test, with the use of Statistica software.
21. G. G. Klaus and M. M. Harnett, *Eur. J. Immunol.* **20**, 2301 (1990).
22. Purified B cells were stimulated with $F(ab')_2$ goat anti-mouse IgM (25 μg/ml) at 37°C and the reaction was stopped at different times by placement of cells on ice. Cells were lysed for 20 min at 4°C in lysis buffer containing 1% NP-40; 20 mM triethanolamine (pH 7.8); 150 mM NaCl; 500 mM EDTA; 100 mM orthovanadate; and a mixture of protease inhibitors-PMSF, pepstatin, leupeptin, and antipain at standard concentrations (*5, 26*). For the analysis of Btk phosphorylation, Btk was precipitated from cell lysates with a rabbit polyclonal antiserum raised against a peptide corresponding to amino acids 71 to 93 of Btk. The specificity of the immunoprecipitation was controlled by incubation of cell lysates with the antiserum to Btk in the presence of the immunogenic peptide for 1 hour. The phosphorylation of Btk was determined by protein immunoblot analysis of immunoprecipitates with the antibody to phosphotyrosine 4G10 and was detected with ECL reagents (Amersham). All samples contained equal amount of immunoreactive protein as determined by immunoblot analysis of immunoprecipitates with antibodies to Btk.
23. L. Yao, Y. Kawakami, T. Kawakami, *Proc. Natl. Acad. Sci. U.S.A.* **91**, 9175 (1994).
24. M. L. Lindsberg *et al.*, *J. Immunol.* **147**, 3774 (1991).
25. R. M. Marais and P. J. Parker, *Eur. J. Biochem.* **182**, 129 (1989).
26. A. Tarakhovsky *et al.*, *Nature* **374**, 467 (1995).
27. R. R. Rickert, K. Rajewsky, J. Roes, *ibid.* **376**, 352 (1995).

28. We thank A. Benner, C. Uthoff-Hachenberg, and C. Göttlinger for technical assistance; P. Parker for the antibodies to PKC-βII; R. Kühn for E14.1 ES cells; K. Rajewsky for support and helpful discussions; and R. Pelanda, R. Rickert, R. Torres, and N. Wagner for critical reading of the manuscript. Supported by the Bundesministerium für Forschung und Technologie (BMFT grant 0316150A) (S.St.), the Deutsche Forschungsgemeinschaft through Sonderforschungsbereich 243 (A.T.), and the Fonds der Chemischen Industrie (C.S.).

10 May 1996; accepted 27 June 1996